Genomic Landscape of Lymphatic Malformations: A Case Series and Response to the PI3Kα Inhibitor Alpelisib in an N-of-One Clinical Trial

Montaser F. Shaheen[1,2,*,†], Julie Y. Tse[3,*,†], Ethan S. Sokol[3], Margaret Masterson[4,5], Pranshu Bansal[6,7], Ian Rabinowitz[6,7], Christy A. Tarleton[6,8], Andrey S. Dobroff[6,8], Tracey L. Smith[9,10], Thèrése J. Bocklage[6,11], Brian K. Mannakee[1,12], Ryan N. Gutenkunst[1,13], Joyce E. Bischoff[14,15], Scott A. Ness[6,8], Gregory M. Riedlinger[4,16], Roman Groisberg[4,17], Renata Pasqualini[9,10,†], Shridar Ganesan[4,17,*,‡], and Wadih Arap[6,18,*,‡]

[1]University of Arizona Cancer Center; Tucson, AZ 85719.

[2]Division of Hematology/Oncology, Department of Medicine, University of Arizona College of Medicine; Tucson, AZ 85724.

[3]Foundation Medicine, Inc.; Cambridge, MA 02141.

[4]Rutgers Cancer Institute of New Jersey; New Brunswick, NJ 08901.

[5]Department of Pediatrics, Rutgers Robert Wood Johnson Medical School; New Brunswick, NJ 08901.

[6]University of New Mexico Comprehensive Cancer Center; Albuquerque, NM 87131.

[7]Division of Hematology/Oncology, Department of Internal Medicine, University of New Mexico School of Medicine; Albuquerque, NM 87131.

[8]Division of Molecular Medicine, Department of Internal Medicine, University of New Mexico School of Medicine; Albuquerque, NM 87131.

[9]Rutgers Cancer Institute of New Jersey; Newark, NJ 07103.

[10]Division of Cancer Biology, Department of Radiation Oncology, Rutgers New Jersey Medical School; Newark, NJ 07103.

[11]Department of Pathology, University of Kentucky College of Medicine and Markey Cancer Center; Lexington, KY 40536.

[12]Department of Epidemiology and Biostatistics, Mel and Enid Zuckerman College of Public Health, University of Arizona; Tucson, AZ 85724.

[13]Department of Molecular and Cellular Biology, College of Science, University of Arizona; Tucson, AZ 85721.

[14]Vascular Biology Program, Boston Children's Hospital; Boston, MA 02115.

[15]Department of Surgery, Harvard Medical School; Boston, MA 02115.

[16]Department of Pathology, Rutgers Robert Wood Johnson Medical School; New Brunswick, NJ 08901.

[17]Division of Medical Oncology, Department of Medicine, Rutgers Robert Wood Johnson Medical School; New Brunswick, NJ 08901.

[18]Division of Hematology/Oncology, Department of Medicine, Rutgers New Jersey Medical School, Newark, NJ 07103.

*Corresponding authors. Correspondence should be addressed to Dr. Wadih Arap, 185 South Orange Ave. B-1121, Newark, NJ 07103, phone: 973-972-0366, E-mail: wadih.arap@rutgers.edu; Dr. Montaser F. Shaheen, E-mail: shaheenm@email.arizona.edu; Dr. Julie Y. Tse, E-mail: jtse@foundationmedicine.com; or Dr. Shridar Ganesan, E-mail: ganesash@cinj.rutgers.edu.

†Montaser F. Shaheen and Julie Y. Tse contributed equally to this work.

‡Renata Pasqualini, Shridar Ganesan, and Wadih Arap jointly supervised this work.

Conflict of interest statement: M.F.S. reports personal fees from Illumina, BMS, and Qiagen (outside of the submitted work). J.Y.T., E.S.S., and B.K.M. are employees of Foundation Medicine, Inc., a wholly owned subsidiary of Roche, and they own equity in Roche. S.G. has consulting agreements with Merck, Roche, Novartis, Foundation Medicine, EQRX, Foghorn

Therapeutics, Silagene, and KayoThera and owns equity in Silagene; his spouse is an employee of Merck and owns equity in Merck (all outside of the submitted work). R.G. reports research funding/grant support for clinical trials (to his institution) from Regeneron, BMS, Merck/EMD Serano, Amgen, Roche/Genentech, Philogen; consulting/advisory board fees from Regeneron; and speaker fees for Deciphera (all outside of the submitted work). R.P. and W.A. are founders and equity stockholders of PhageNova Bio and of MBrace Therapeutics; R.P. is a paid consultant for PhageNova Bio and MBrace Therapeutics and also serves as the Chief Scientific Officer of PhageNova Bio and a member of the board for MBrace Therapeutics (all outside of the submitted work). For R.G., R.P., S.G., and W.A., these arrangements are managed in accordance with the established institutional conflict of interest policies of Rutgers, The State University of New Jersey. The remaining authors have declared no potential competing interests.

KEYWORDS: lymphatic malformations, genomics, NGS, PI3Kα

ABSTRACT

Background: Lymphatic malformations (LMs) often pose treatment challenges due to a large size or a critical location that could lead to disfigurement, and there are no standardized treatment approaches for either refractory or unresectable cases.

Methods: We examined the genomic landscape of a patient cohort of LMs (n=30 cases) that underwent comprehensive genomic profiling (CGP) using a large-panel next generation sequencing (NGS) assay. Immunohistochemical analyses were completed in parallel.

Results: These LMs had low mutational burden with hotspot *PIK3CA* mutations and *NRAS* mutations being most frequent, and mutually exclusive. All LM cases with Kaposi sarcoma-like (kaposiform) histology had *NRAS* mutations. One index patient presented with subacute abdominal pain and was diagnosed with a large retroperitoneal lymphatic malformation harboring a somatic *PIK3CA* gain-of-function mutation (H1047R). The patient achieved a rapid and durable complete response to the PI3Kα inhibitor alpelisib within the context of a personalized N-of-1 clinical trial (NCT03941782). In translational correlative studies, canonical PI3Kα pathway activation was confirmed by immunohistochemistry and human LM-derived lymphatic endothelial cells carrying an allele with an activating mutation at the same locus were sensitive *in vitro* to alpelisib in a concentration-dependent manner.

Conclusions: Our findings establish that LM patients with conventional or kaposiform histology have distinct, yet targetable, driver mutations.

Funding: R.P. and W.A. are supported by awards from the Levy-Longenbaugh Fund. S.G. is supported by awards from the Hugs for Brady Foundation. This work has been funded in part by the NCI Cancer Center Support Grants (CCSG; P30) to the University of Arizona Cancer Center (CA023074), the University of New Mexico Comprehensive Cancer Center (CA118100), and the

89 Rutgers Cancer Institute of New Jersey (CA072720). B.K.M. was supported by National Science
90 Foundation via Graduate Research Fellowship DGE-1143953.

91 **Clinical trial number:** NCT03941782

92

93

94

INTRODUCTION

Vascular anomalies, including lymphatic malformations (LMs), are usually diagnosed in children or young individuals and they can present as either isolated lesions or as part of somatic or congenital syndromes. In general, LMs are managed by sclerotherapy, laser, or surgical interventions when there is an indication for therapy[1]. In certain cases, LMs can attain large sizes or involve critical locations, which poses treatment challenges such as the possibility of disfigurement. Genomic sequencing has demonstrated a somatic clonal origin for a number of non-malignant growth conditions including LMs. Activating *PIK3CA* mutations have been reported in most pediatric patients with isolated or syndromic LMs[2]. This finding has led to the use of mammalian target of rapamycin (mTOR) inhibitors for systemic therapy of unresectable LMs, given that mTOR is a molecule downstream of the PI3K pathway[3]. However, only a subset of patients responded, and the treatment can have substantial side-effects. PI3K inhibitors have also been reported as being effective in treatment of children with diseases in the *PIK3CA*-related Overgrowth Spectrum (termed PROS), but the efficacy of alpelisib in isolated sporadic LMs is not at all clear. Similarly, it is not as yet clear which oncogenic drivers, if any, are present in LMs with wild-type *PIK3CA* alleles.

To define the spectrum of genomic alterations and lesions present in LMs, here we have analyzed a patient cohort of LMs (n=30 cases) assayed by clinical-grade genomic sequencing. Pathogenic activating mutations in *PIK3CA* and *NRAS* were the most common genetic alterations found. Strikingly, the *PIK3CA* and *NRAS* mutations were mutually exclusive with *NRAS* mutations being greatly enriched in LMs with kaposiform morphology. We have also performed an N-of-1 trial of the PI3Kα inhibitor alpelisib in a young man with an activating *PIK3CA* point mutation, presenting with a giant (unresectable) retroperitoneal and pancreatic

LM, who had a dramatic and prolonged response to the drug lasting years, and we present confirmatory translational correlates *in vitro*.

RESULTS

Mutational Landscape and Histopathology of Lymphatic Malformations

A set of thirty cases of LMs (from 30 individual patients) were assayed with genomic profiling at Foundation Medicine, Inc. (Cambridge, MA). Twenty-eight cases were sequenced using hybrid-capture next-generation sequencing (NGS) targeting exons of 300+ cancer genes and select introns of 36 genes. Two other cases were sequenced using hybrid-capture based DNA sequencing targeting exons of 406+ cancer genes and select introns of 36 genes, plus RNA sequencing of 265 genes for rearrangement calling. The patients were predominantly pediatric age (median 9-year-old; range, 1-year-old to 45-years-old), with a slight female predominance (17 females, 57% to 13 males, 43%). Seven patients had a documented history of prior treatment with an mTOR inhibitor, such as sirolimus. Seven patients (23%) carried clinical diagnoses of overgrowth syndromes including Congenital Lipomatous Overgrowth with Vascular, Epidermal, and Skeletal anomalies (termed CLOVES), Klippel-Trenaunay Syndrome, and PTEN-like hamartoma syndrome. Twelve patients (40%) had multifocal disease and eight patients had involvement of bone and visceral sites (**Table 1**). Expert histopathological review showed that only four (13%) had kaposiform morphology, while 26 (87%) had conventional histology. The estimated histopathologic purity ranged from 10% to 70% (median 20%).

145 **Table 1: Clinical and histological features of lymphatic malformation cohort**

Patient	Age range (years)	Sex	Clinical syndrome	Localized vs. multifocal	Location of LM(s)	Specimen type	LM histology	*PIK3CA* or *NRAS* alteration	% VAF
1	6-10	M	CLOVES	Multifocal	Superficial soft tissues	Excision	Conventional	*PIK3CA* E542K	14
2	0-5	F		Localized	Superficial soft tissues	Excision	Conventional	*PIK3CA* E542K	7
3	0-5	F		Localized	Superficial soft tissues	Excision	Conventional	*PIK3CA* H1047R	11
4	16-20	M		Localized	Superficial soft tissues	Excision	Conventional	*PIK3CA* H1047R	4
5	16-20	M		Localized	Superficial soft tissues	Excision	Conventional	*PIK3CA* H1047L	4
6	6-10	F	Klippel-Trenaunay	Localized	Superficial soft tissues	Excision	Conventional	*PIK3CA* H1047R	9
7	6-10	M		Localized	Visceral	Core biopsy	Conventional	*PIK3CA* E545K	7
8	0-5	F		Localized	Superficial soft tissues	Excision	Conventional	*PIK3CA* C420R	5
9	21-25	M		Localized	Visceral	Incisional biopsy	Conventional	*PIK3CA* H1047R	4
10	16-20	F	PTEN-like hamartoma	Localized	Superficial soft tissues	Excision	Conventional	*PIK3CA* H1047R	3
11	0-5	F	CLOVES	Multifocal	Superficial soft tissues	Excision	Conventional	*PIK3CA* E545K	12
12	0-5	M		Multifocal	Superficial soft tissues	Excision	Conventional	*PIK3CA* H1047R	2
13	0-5	F		Localized	Superficial soft tissues	Excision	Conventional	*PIK3CA* E542K	6
14	0-5	M		Localized	Superficial soft tissues	Excision	Conventional	*PIK3CA* H1047R	5
15	0-5	F		Localized	Superficial soft tissues	Excision	Conventional	*PIK3CA* E545K	1
16	11-15	F		Multifocal	Visceral	Excision	Conventional	*PIK3CA* C420R	14
17	0-5	F	CLOVES	Multifocal	Superficial soft tissues	Excision	Conventional	*PIK3CA* C420R	38
18	16-20	F	CLOVES	Localized	Superficial soft tissues	Excision	Conventional	*PIK3CA* E453K	32
19	6-10	F	CLOVES	Multifocal	Superficial soft tissues	Excision	Conventional	*PIK3CA* H1047L	15
20	6-10	M		Localized	Superficial soft tissues	Excision	Conventional	*PIK3CA* H1047R	5
21	6-10	F		Multifocal	Visceral	Excision	Kaposiform	*NRAS* Q61R	5
22	6-10	M		Multifocal	Superficial soft tissues	Excision	Kaposiform	*NRAS* Q61R	5
23	6-10	F		Multifocal	Visceral	Excision	Kaposiform	*NRAS* Q61R	1
24	41-45	M		Multifocal	Visceral	Core biopsy	Conventional	*NRAS* Q61R	6
25	6-10	F		Localized	Superficial soft tissues	Core biopsy	Kaposiform	*NRAS* Q61R	14
26	16-20	M		Multifocal	Superficial soft tissues	Excision	Conventional	WT	NA
27	21-25	M		Localized	Bone	Core biopsy	Conventional	WT	NA
28	0-5	M		Multifocal	Superficial soft tissues	Excision	Conventional	WT	NA
29	11-15	F		Localized	Superficial soft tissues	Excision	Conventional	WT	NA
30	6-10	F		Localized	Superficial soft tissues, bone	Biopsy	Conventional	WT	NA

146

147 Key: VAF – variant allele frequency of *PIK3CA* or *NRAS*; CLOVES – congenital lipomatous overgrowth,
148 vascular anomalies, epidermal nevi, and skeletal anomalies; NA - not applicable

Mutational profiling showed that these LMs had uniformly low mutational burden (median, zero mutations/Mb; range, 0-2.6 mutations/Mb), and none had evidence of microsatellite instability. The most common mutations were activating mutations in *PIK3CA*, seen in 20 (67%), and activating *NRAS* mutations, seen in 5 (17%) (**Figure 1A, B**). The *PIK3CA* mutations included both hotspot mutations in the helical domain and in the kinase domain[4]. The *NRAS* mutations all altered the known hotspot at residue glutamine 61 (Q61) in the phosphorylation binding loop. Of the five patients (17%) with no alterations in *PIK3CA* and *NRAS*, one case (Patient #29; **Table 1**) had an activating *GOPC-ROS1* fusion (**Figure 1C**) with a *ROS1* missense point mutation. Similar *GOPC-ROS1* fusions have been reported in pediatric gliomas in the setting of microdeletion of chromosome 6q22[5] and, have also been found in adult lung cancer[6].

The variant allele frequencies (VAF) of the *PIK3CA* and *NRAS* mutations were relatively low (median, 6%; range, 1-38%), compatible with relatively low histopathologic estimated percentage of tumor nuclei (%TN) to overall cellular nuclei (median, 20%; range, 10 to 70%). These results suggest that the *PIK3CA* and *NRAS* mutations were likely clonal, but in the setting of relatively low tumor purity in the specimens.

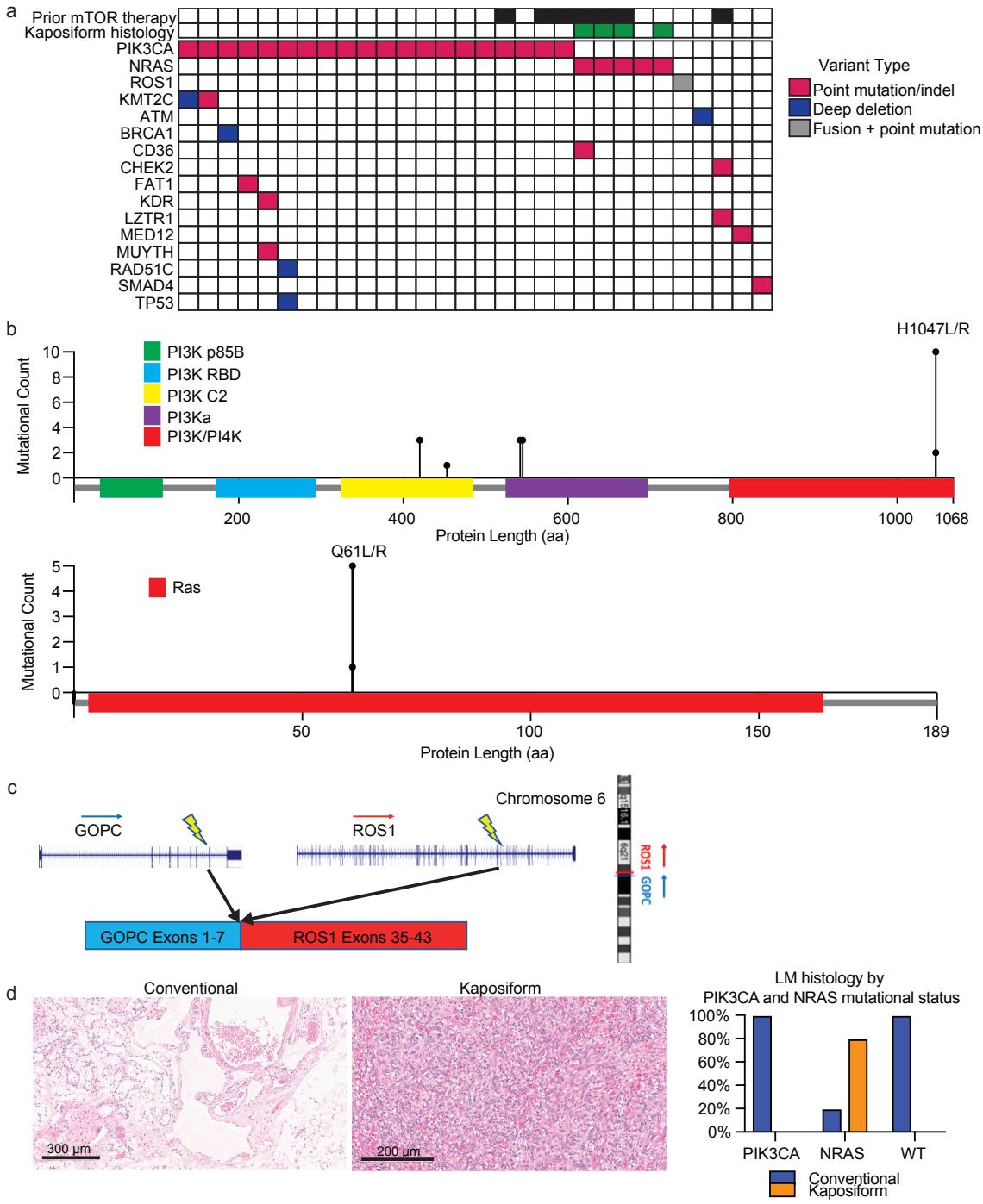

Fig. 1. Mutational Landscape and Histopathology of Lymphatic Malformations. (A) Oncoprint showing mutational landscape of 30 LM samples sequenced. **(B)** Lollipop plot showing spectrum of *PIK3CA* and *NRAS* mutations in this cohort. **(C)** Schema showing details of *GOPC-ROS1* fusion identified in an *NRAS* and *PIK3CA* wild-type LM. **(D)** Representative histologic images for LMs with conventional and kaposiform histology. The relative frequencies of *PIK3CA* and *NRAS* mutations in the two histologic variants are plotted.

Enrichment of *NRAS* Mutations in Lymphatic Malformations with Kaposiform Features

Histopathological analysis of the lesions by an expert dermatopathologist (J.Y.T.) identified that four (13%) of the analyzed specimens had kaposiform histopathological features with highly cellular, clustered, or sheet-like, proliferation of spindled lymphatic cells admixed with dilated thin-walled lymphatic vessels **(Figure 1D**). The remaining 26 lesions (87%) had conventional histopathological features of classic LM, with proliferation of dilated, thin-walled lymphatic vessels with or without luminal proteinaceous material. Lymphatic phenotype of the cells was confirmed by immunopositivity for PROX1 or D2-40. Of the conventional histology LM cases (n=26), twenty (77%) had a *PIK3CA* mutation, while one (4%) had a *NRAS* mutation, and five (19%) were wild-type for both genes, including a single-case with a *GOPC-ROS1* genetic fusion. Notably, all four cases of LM with kaposiform features had an activating *NRAS* mutation, consistent with enrichment of *NRAS* mutation (p=0.00018) and lack of *PIK3CA* mutation in this histology (p=0.0046). The lone *NRAS*-mutant LM with conventional histology was a small core needle-biopsy specimen of a large visceral tumor, raising the possibility that the histopathologic features of the sampled tissue may not have been representative of the entire lesion due to the histologic spatial heterogeneity often seen in LMs with kaposiform histology. Additional histopathologic features were assessed, including altered adipose tissue, muscularized blood vessels, vascular endothelial cell atypia, and inflammation; no statistical significance was identified between the four *NRAS*-mutant LM cases and the remainder of the patient cohort.

Case Report and N-of-One Clinical Trial Results

One of the conventional histology LMs was a male (age range 21-25 years) with no significant medical or family history who presented with subacute abdominal pain (Patient #9, **Table 1**). He was hospitalized and his exam revealed a distended abdomen that was tender to palpation. A computed tomography exam revealed a large solid mass based on the retroperitoneal area and

the pancreas (**Figure 2A**), and a neoplastic process was suspected. A core needle biopsy was attempted but yielded no definitive tissue diagnosis. An open laparoscopic surgical biopsy was performed and revealed a vascular tumor with features of a giant retroperitoneal and pancreatic LM (**Figure 2 D,E**). After discussing a surgical approach, the patient and the surgical team decided not to proceed due to the complexity of surgical resection and associated risks. The tissue was submitted for NGS to identify potential biomarkers for targeted therapy.

Clinical grade sequencing of the biopsy sample from Patient #9 uncovered a single point activating mutation in *PIK3CA* (H1047R). All other genes in the panel were wild-type except for another unit of the PI3K complex (*PIK3C2B*) that showed a variant (R458Q) of unknown significance (VUS). To confirm activation of the PI3Kα pathway, we performed immunohistochemistry (IHC) staining of the downstream targets (P-AKT and P-6S), and, as predicted, these phosphorylation events were detected in the lining cells of the abnormal lymphatic channels (**Figure 2 F,G**).

Based on the genomic profile, we designed and offered this young man a single-patient (N-of-One) personalized clinical trial of the PI3Kα inhibitor alpelisib (NCT03941782), which at the time was still investigational (non-FDA approved). Screening procedures included an echocardiogram that revealed an ejection fraction (EF) of 47%. A cardiac MRI confirmed a low EF with no infiltrative process or other abnormalities. Paradoxically, the patient was completely asymptomatic from a cardiac standpoint and he was able to run two miles on a daily basis. We hypothesized that the decreased EF, in the absence of accompanying clinical signs or symptoms of heart failure, was likely artefactual due to hemodynamic changes related to the very large circulatory volume sequestration in his abdomen.

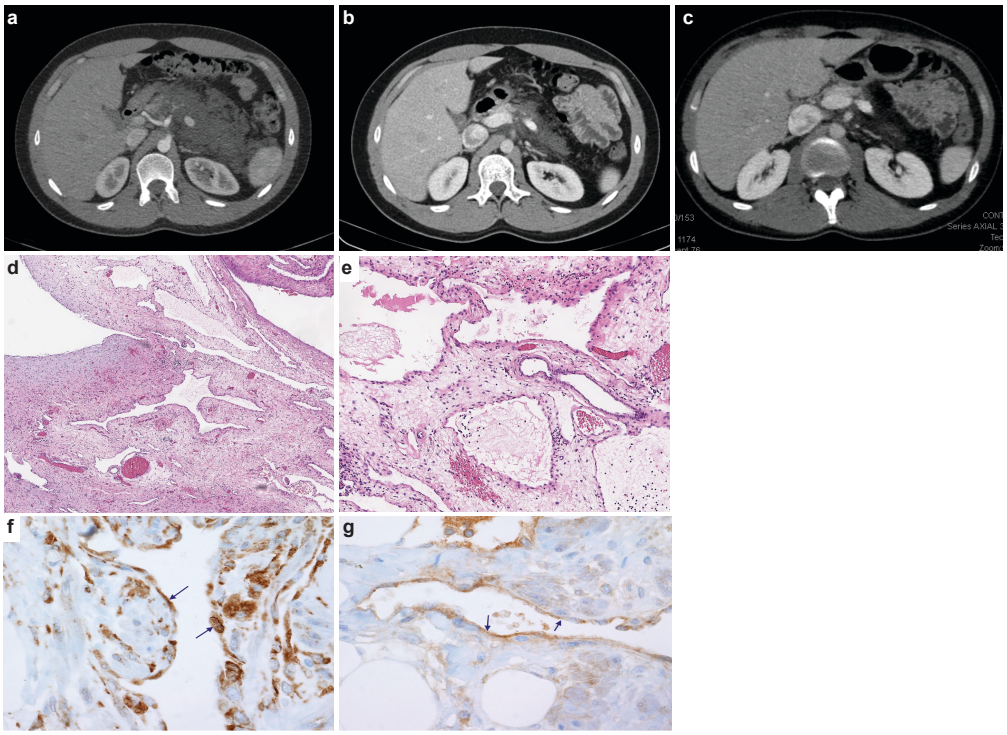

Fig. 2. Imaging and histological analysis of LM patient. (A) Baseline CT abdomen scan at the time of presentation demonstrating a large retroperitoneal/pancreatic LM. **(B)** CT abdomen scan 6 weeks after the initiation of alpelisib. **(C)** CT abdomen scan one year into the trial. **(D and E)** Hematoxylin and eosin (H&E)-stained photomicrographs of the LM showing dilated lymphatic channels percolating through visceral fat and associated patchy lymphocytic inflammation (4x and 10x, respectively). **(F)** Immunohistochemistry utilizing an anti-P-6S antibody demonstrates PI3Kα pathway activation within the channels' lining cells. **(G)** Anti-P-AKT positivity in the lining endothelium of lymphatic channels as well.

The patient was started on alpelisib daily dose of 350 mg orally[7] and he reported regression of his abdominal bulge within a few days. He reported no adverse events and was closely monitored for hyperglycemia. Repeated echocardiogram two months later showed normalization of the EF. A CT scan of the abdomen done six weeks into the trial revealed remarkable shrinkage of the LM (**Figure 2B**). Follow-up CT scans showed progressive reduction until complete response at one year of trial initiation (**Figure 2C**). The patient continued to do well on maintenance alpelisib for 2 years with no evidence of progression. After two years, alpelisib was discontinued due to theoretical concerns about long-term adverse impact on vascular

239 homeostasis. Unfortunately, the mass recurred after a few weeks so the patient was resumed
240 on alpelisib with a second deep partial response, which is still ongoing for over three years.

241

242 **Alpelisib Inhibits Primary PI3Kα-mutant Lymphatic Malformation-derived Endothelial**
243 **Cells**

244 We have also investigated the concentration-dependent effects of alpelisib on lymphatic
245 malformation-lymphatic endothelial cells (LM-LECs) isolated from a surgically resected
246 specimen[8]. Targeted sequencing of DNA from LM-LECs identified a somatic missense mutation
247 in *PIK3CA* (H1047L), the same locus altered in our alpelisib-treated patient and the site of half
248 of the *PIK3CA* alterations in the LM cohort studied (**Table 1**). In addition, a nonsense mutation
249 of the regulatory PI3K unit *PIK3R3* (R309*) was also detected in the CD31-positive LM-LECs
250 and CD31-negative non-endothelial cells isolated from the same LM, indicating its germline
251 origin[8]. We investigated the effect of alpelisib on the growth of LM-LECs and a concentration-
252 dependent response curve was observed (**Figure 3**). The IC_{50} of alpelisib against LM-LECs was
253 empirically determined *in vitro* to be 4.72 x 10^{-9} M at 24 hours. This *in vitro* translational model
254 confirms the sensitivity of LM-derived human cells containing a target $H1047^{R}/_{L}$ mutation to
255 alpelisib.

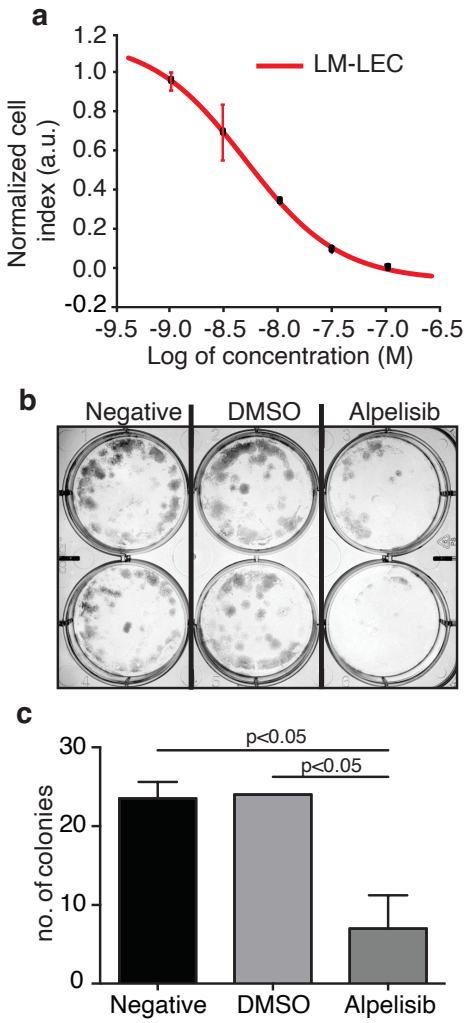

Figure 3. Alpelisib reduces LM-LEC viability. (A) Logarithmic dose response curve of alpelisib was performed using the xCELLigence RTCA system. 1, 3, 10, 30 and 100 nM (5 replicates/concentration) of alpelisib were used to determine the concentration-response curve. The alpelisib half maximal inhibitory concentration (IC_{50}) was calculated for LM-LEC at 24 h after treatment as 4.72×10^{-9} M. **(B**) Illustrative picture of LM-LEC clonogenic plaques at 24 h after alpelisib treatment (4.72×10^{-9} M). Negative, no treatment; dimethyl sulfoxide (DMSO), vehicle control. Experiments were performed two times with similar results. LM-LEC colonies were stained with crystal violet (0.3%). **(C)** Colony count 24 h after alpelisib treatment (4.72×10^{-9} M).

Refined Genomic and Sequencing Analyses

We performed whole-genome sequencing (WGS) on paired LM/germline DNA from our index patient to explore the mutational profile beyond the genes that were probed in the Clinical Laboratory Improvement Amendments (CLIA)-approved clinical sequencing assay. The *PIK3CA*

H1047R mutation was identified with a Variant Allele Frequency (VAF) of 11%. This finding is consistent with the ≤10 % rate of mutant cells, and low tumor cellularity of LMs with *PIK3CA* mutation[2]. Few other somatic coding mutations were identified in the LM tissue (**Supplementary Table 1**).

To gain further molecular mechanistic insight, we have also performed RNA-seq studies to identify gene expression patterns within the LM sample from our index patient. RNA-seq data of biopsy samples from Patient #9 (n=2 samples; Group A) was compared to several normal human control tissue samples from bladder, colon, kidney, and salivary gland (n=4, one sample per each tissue; Group B). By using an arbitrary cut-off of at least 2-fold up or down with adjusted *p*-values of 0.05 or less, we identified 668 up-regulated and 850 down-regulated genes. Several of the most highly induced genes, *CHI3L1*, *GPX1*, *PLIN1*, *PLIN4* and *JAK3*, have been linked to enhanced growth or cell survival in other tumor types[9-13]. Finally, a preliminary Gene Ontogeny (GO) analysis of Patient #9 LM revealed enrichment of mRNA of genes involved in vascular development, cell motility, inflammatory response, positive regulation of response to stimuli, blood vessel morphogenesis among others; notably, the kinase *JAK3* gene was one of the highest expression mRNAs in the LMs compared to normal tissue controls (data not shown).

DISCUSSION

Here we report the mutational landscape of a patient cohort of LMs (n=30 cases) which underwent comprehensive genomic profiling. We have confirmed prior reports that hotspot activating mutations in *PIK3CA* are common driver events in these lesions, seen in 20 (67%) of these cases. Interestingly *NRAS* mutations were seen in an additional 5 (17%) cases and were

particularly enriched in LMs with a kaposiform histopathology. This finding suggests that LMs with kaposiform features may represent a different pathologic entity [14,15]. As a caveat, for the one *NRAS* mutant LM with classic histology, the histologic classification was based on a small biopsy, and it is certainly possible that kaposiform histology was present in the large visceral LM but not captured by the limited sampling by core needle biopsy. Importantly, three of the five patients (60%) with *NRAS* mutant LMs had failed treatment with sirolimus prior to NGS. There are reports that some *NRAS*-mutant LMs may respond to treatment with MEK inhibitors[16], suggesting this may be an option for LMs with kaposiform features.

Of the 5 cases without either *PIK3CA* or *NRAS* mutations, all of classic histology, a single case had a known pathogenic in-frame *GOPC-ROS1* genetic fusion predicted to have an intact ROS1 kinase domain and thus potentially function as the driver. Similar *GOPC-ROS1* fusions have been seen in pediatric gliomas and adult lung cancers and may be sensitive to ROS1 inhibitors[5,6]. These data suggest that most LMs may have a potentially actionable driver mutation, with *PIK3CA* mutations dominating LMs with conventional histology and *NRAS* mutations predominantly or exclusively seen in the minor subset of LMs with kaposiform features. It is possible that the other *NRAS* and *KRAS* wild-type LMs may also have oncogenic alterations in other members of the *PIK3CA* or MAPK signaling pathway members that were not profiled by targeted sequencing strategies. Comprehensive NGS analysis of LMs with *PIK3CA* and *NRAS* wild-type may be required to identify any potential actionable driver mutations. In patients without solid LM tissue available for NGS, liquid biopsy--or NGS performed on circulating tumor DNA (ctDNA) in peripheral blood--may be a possible solution for LMs, which are innately associated with the vascular system and thus potentially “shedding” ctDNA into the peripheral blood.

To illustrate the potential for therapeutic intervention of the target mutations identified, we performed an N-of-1 trial of alpelisib in one young adult index patient with a giant retroperitoneal and pancreatic LM with conventional histological features and a gain-of-function H1047R somatic *PIK3CA* mutation. Our index patient experienced a rapid, complete, and durable clinical response with this small molecule PI3Kα inhibitor. Given the high frequency of *PIK3CA* mutations in pediatric LMS[2], this finding suggests that alpelisib may be highly effective for systemic, non-surgical treatment approach to this class of disorders. Furthermore, the lack of toxicity to alpelisib in our case is promising in terms of a potential future treatment of young patients with LMs. Our patient did not experience increases in glucose levels, consistent with reported lack of alpelisib-induced hyperglycemia in most pediatric patients with PROS[17,18]. In this prior series, only one patient developed new-onset hyperglycemia and this was controlled by dietary modification[17]. These findings suggest that the effect of alpelisib on inducing hyperglycemia might perhaps be less of a concern in younger patients, who may have more robust glucose homeostasis, compared with older patients who may already have subclinical insulin-resistance.

Ultimately, we decided to hold alpelisib after two years of complete radiological response, and unfortunately the LM relapsed but the patient still achieved a major partial response on the second challenge with alpelisib. This result suggests that PI3Kα inhibitors do not completely eradicate all LM-initiating cells, and they may need to be given long-term (in our young index patient case, perhaps over decades) in *PIK3CA* mutant LMs for sustained control. This class of drugs can also be envisioned to be utilized in a neoaduvant approach to render large cases resectable. Our patient declined surgery after initial response and he continues on alpelisib for several years. Acquired resistance mechanisms to PI3Kα inhibitors have been reported, due to other associated compensatory or bypassing mutations such as ones involving *RAS* oncogene[19]

or *PTEN* tumor suppressor gene[20], and these may conceivably arise in these patients with longer follow up over time. Deftly balancing the potential benefits of continuing treatment with the potential for drug resistance mechanisms will require monitoring for both actionable known and novel mutations through NGS of LM tissue samples or liquid biopsy.

In a series of pediatric patients with LMs, Luks et al. identified *PIK3CA* gene mutations in patients with sporadic LMs in 16 out of 17 patients (94%) or syndromic LMs such as the Klippel-Trenaunay syndrome in 19 out of 21 patients (90%), fibro-adipose vascular anomaly in 5 out of 8 patients (63%), along with the CLOVES syndrome in 31 out of 33 patients (94%)[2]. H1047R was one of the top two most frequently encountered hotspot mutations in this series. Venot et al. reported a single arm clinical trial of alpelisib in 19 patients with pediatric PROS including CLOVES[17]. Alpelisib treatment induced clinical responses in all patients, including improvement of cardiac EF as seen in our index patient. Of note, alpelisib induced responses in patients who did not respond to prior treatment with mTOR inhibitors, such as rapamycin, similar to observations in *KRAS* mutant oncology patients[21]. Small clinical series have shown that mTOR inhibition can induce responses in a subset of unselected advanced LMs, with observed response rates of ~50-60%[22]. The on driver-oncoprotein activity, higher response rates, and tolerability suggests alpelisib may be more effective than mTOR inhibitors in this setting. It is tempting to speculate that a wide variety of *PIK3CA* mutant somatic overgrowth conditions[23] may be amenable to medical treatment with FDA-approved PI3Kα inhibitors, either as neo-adjuvant treatment in potentially resectable cases, or as primary treatment in unresectable cases[7,20,24-26].

Furthermore, in our Whole Genome Sequencing (WGS) analysis, we identified only a few somatic variants within protein-coding genetic sequences (**Supplementary Table 1**) beyond

what was reported in the cancer gene panel (**Table 1**). The low frequency of somatic mutations is consistent with findings in other low-grade pediatric tumors[27]. In addition to detecting the *PIK3CA* H1047R mutation, this WGS confirmed the variant detected by the cancer gene panel in the *PIK3C2B* gene and demonstrated that it was germline. Although this in *PIK3C2B* variant has not been characterized and may be a benign polymorphism, this finding raises the issue of whether other alterations in the pathway may cooperate with activating mutations of *PIK3CA* to induce cell proliferation. The low VAF driver mutations in tissue derived from LMs is likely due to the fact that most pathological tissue is composed of reactive stromal elements while the clonal cells represent a relatively small portion (presumably the lymphatic channel-lining endothelial cells). Consistent with this observation, in the alpelisib-treated index patient, we observed most intense activation of the PI3Kα pathway in these lymphatic channel-lining endothelial cells (**Figure 2 F,G**). The high representations of pathways associated with vascular development, cell motility, inflammatory response, positive regulation of response to stimuli, blood vessel morphogenesis in our gene expression analysis is consistent with a mechanistic hypothesis that most of the lesion represents an intense reactive response to the (presumably) clonal LM-LECs, although the appropriate comparator control tissues for these lesions is not clear.

Evidence is accumulating that a variety of “non-malignant” syndromes associated with abnormal tissue growth may be driven by underlying alterations in classic oncogenes[28]. *PIK3CA* mutations are seen not only in LMs but other vascular anomalies, highlighting the role of *PIK3CA* activation in angiogenesis, lymphangiogenesis and vascular neoplasms[29-31 32]. Endometriosis, uterine fibroids and seborrheic keratoses all have been found to harbor mutations in cancer related genes[33-37]. These findings suggest that targeted therapies being developed for invasive cancers may also be active in proliferative lesions that are not classified as invasive cancers that harbor the targeted alteration.

In summary (**Figure 4**), we find that the majority of LMs have driver mutations that are potentially targetable. LMs with classic histology mostly have *PIK3CA* mutations that may respond to alpelisib. LMs with kaposiform histopathology are enriched in *NRAS* mutations, and studies are required to determine if these may respond to clinically available MEK inhibitors. LMs that are wild-type for *PIK3CA* and *NRAS* may have other actionable alterations, such as the *GOPC-ROS1* fusion seen in our series and may require more comprehensive genomic analyses to identify them. Systemic treatment with targeted therapy aimed at the driver mutation in LMs may be an option for some patients who are not controlled by surgery and other conventional treatments.

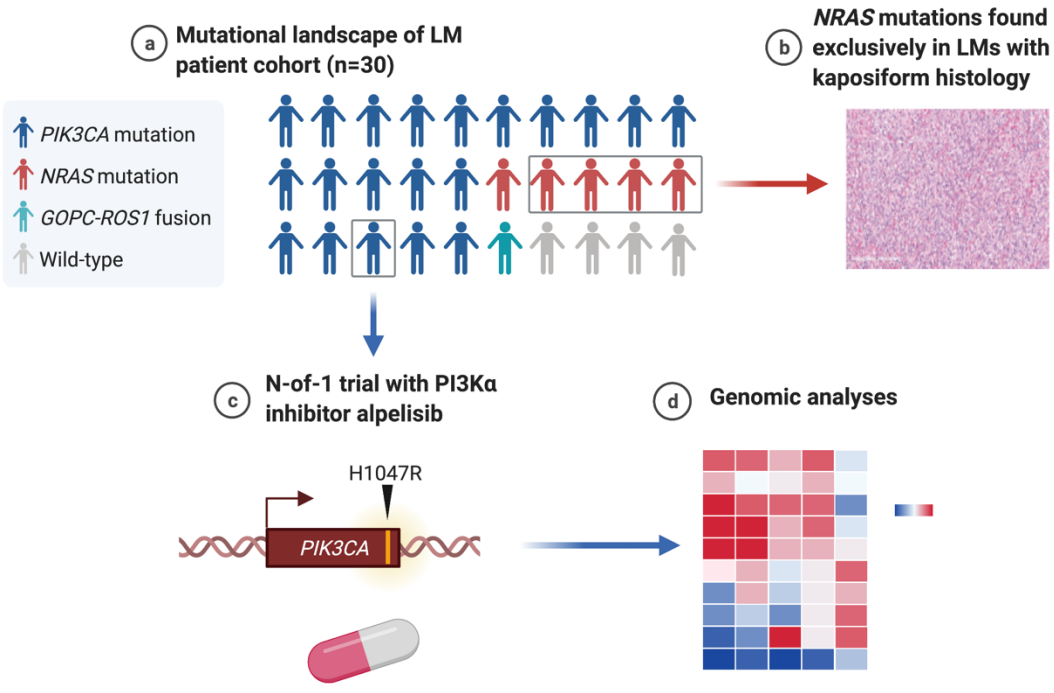

Figure 4. Graphical summary of the mutations found in genomic analysis of LM patient cohort (Created with BioRender.com). (A) The majority of LMs have driver mutations that are potentially targetable. **(B)** LMs with *NRAS* mutations had kaposiform histopathology. **(C)** An N-of-1 clinical trial is reported in a patient with a targetable PIK3CA mutation. **(D)** Comprehensive genomic analyses may reveal further actionable molecular insights.

METHODS

Genomics and DNA Sequencing. Hybrid-capture DNA sequencing targeting exons of at least 324 cancer genes and select introns of 36 genes were performed on the patient samples; a subset (n=2) were also analyzed with plus RNA sequencing of 265 genes to improve rearrangement detection. A total of 30 patient samples were sequenced with either the DNA-only assay (n=28; Foundation One CDx, Foundation Medicine; Cambridge, MA) or the DNA+RNA assay (n=2; Foundation One Heme, Foundation Medicine; Cambridge, MA).

Immunohistochemistry. Immunohistochemistry (IHC) was performed on formalin-fixed, deparaffinized, 5-micron thick sections mounted on charged slides. Antibodies to P-AKT (Ser473), and P-6S (Ser240/Ser244) were obtained from Cell Signaling Technology, Danvers, Massachusetts. Diaminobenzidine (DAB) was used as the chromogen and hematoxylin as the counterstain. All stages of staining were carried out on an automated system (Ventana Discovery Research Instrument; Ventana, Tucson, Arizona). Positive and negative controls were appropriately reactive. A surgical pathologist with subspecialty interest in musculoskeletal pathology (T.J.B.) interpreted the results.

LM-LEC Sensitivity to Alpelisib In Vitro. LM-LEC cells were maintained as described [8] and negative for mycoplasma at the time of these studies. Mycoplasma test was performed using the MycoAlert Mycoplasma Detection Kit (Cat # LT07-218, Lonza) following the manufacturer's instructions. Real-time analysis of cell viability was performed by using the xCELLigence system RTCA SP (ACEA Biosciences). Briefly, $5x10^3$ LM-LECs per well were seeded in an E-Plate 96 (ACEA Biosciences) and cell proliferation was recorded hourly. When the cells reached the exponential growth phase, new media containing alpelisib at 1, 3, 10, 30, or 100 nM was added

and alpelisib cytotoxic effect was recorded hourly. IC_{50} was calculated by using the Dose-Response Curve (DRC) function available in the xCELLigence software Version 2.0. Cell index (%) reflects cell viability.

Clonogenic Survival Assays. For the clonogenic survival assay, the LM-LEC were trypsinized, counted and plated in complete growth media on 6-well plates (Falcon) (400 cells/well). Seven days later, alpelisib (at the empirically determined IC_{50} from a standard calibration curve) was added in duplicate wells. After 24 h or 48 h of incubation, cells were fixed and stained in 50% methanol in water containing 0.3% crystal violet to facilitate counting of colonies (≥50 cells).

Statistics. All values are expressed as mean with error bars expressed as SD. For comparison between untreated (negative), DMSO control, and Alpelisib treated LM-LEC cells, the ordinary one-way ANOVA and Tukey's multiple comparisons test with a single pooled variance were used. Statistical analysis was performed using the Graph Pad Prism 7.0d software (GraphPad Software Inc., San Diego, CA, USA). Fisher's exact test was used for categorical data, owing to the sizes of the cohorts. A two-tailed P value of <0.05 was considered to be statistically significant.

Study approval. Approval for this study, including a waiver of informed consent and Health Insurance Portability and Accountability Act waiver of authorization, was obtained from the Western Institutional Review Board (IRB; protocol #20152817). A single-institution personalized clinical protocol to treat the patient with the experimental PI3Kα inhibitor alpelisib was scientifically reviewed by the Protocol Review and Monitoring Committee (PRMC) and approved by the local Institutional Review Board (IRB) of the University of New Mexico Comprehensive

459 Cancer Center. The study (NCT03941782) was conducted in accordance with the protocol,
460 Good Clinical Practice guidelines, and the provisions of the Declaration of Helsinki. CARE
461 reporting guidelines were also used for this patient[38]. The index patient signed an informed
462 written consent form.
463

464 **Author contributions:** Conceptualization: MFS, JYT, ESS, MM, RP, SG, WA; Methodology:
465 MFS, JYT, ESS, PB, IR, CAT, ASD, TLS, TJB, BKM, RNG, JEB, SAN, GMR, RG; Investigation:
466 MFS, JYT, ESS, PB, IR, CAT, ASD, TLS, TJB, BKM, RNG, JEB, SAN, GMR, RG; Visualization:
467 MFS, JYT, ESS, PB, IR, CAT, ASD, TLS, TJB, BKM, RNG, JEB, SAN, GMR, RG; Funding
468 acquisition: MFS, MM, RP, SG, WA; Project administration: MFS, JYT, RP, SG, WA;
469 Supervision: MFS, JYT, RP, SG, WA; Writing – original draft: MFS, JYT, ESS, RP, SG, WA;
470 Writing – review & editing: MFS, JYT, ESS, MM, PB, IR, CAT, ASD, TLS, TJB, BKM, RNG,
471 JEB, SAN, GMR, RG, RP, SG, WA

472

473 **Acknowledgments:** We thank Dr. Kathryn J. Brayer for technical assistance and Dr. Helen
474 Pickersgill (Life Science Editors) for professional manuscript editing services.

475

476 **Funding:** R.P. and W.A. are supported by awards from the Levy-Longenbaugh Fund. S.G. is
477 supported by awards from the Hugs for Brady Foundation. This work has been funded in part by
478 the NCI Cancer Center Support Grants (CCSG; P30) to the University of Arizona Cancer Center
479 (CA023074), the University of New Mexico Comprehensive Cancer Center (CA118100), and the
480 Rutgers Cancer Institute of New Jersey (CA072720). B.K.M. was supported by National Science
481 Foundation via Graduate Research Fellowship DGE-1143953.

482

483

484

References

1. Perkins JA, Manning SC, Tempero RM, Cunningham MJ, Edmonds JL, Jr., Hoffer FA, Egbert MA. Lymphatic malformations: review of current treatment. *Otolaryngol Head Neck Surg.* 2010;142(6):795-803, 803 e791. doi: 10.1016/j.otohns.2010.02.026

2. Luks VL, Kamitaki N, Vivero MP, Uller W, Rab R, Bovee JV, Rialon KL, Guevara CJ, Alomari AI, Greene AK, Fishman SJ, Kozakewich HP, Maclellan RA, Mulliken JB, Rahbar R, Spencer SA, Trenor CC, 3rd, Upton J, Zurakowski D, Perkins JA, Kirsh A, Bennett JT, Dobyns WB, Kurek KC, Warman ML, McCarroll SA, Murillo R. Lymphatic and other vascular malformative/overgrowth disorders are caused by somatic mutations in PIK3CA. *J Pediatr.* 2015;166(4):1048-1054 e1041-1045. doi: 10.1016/j.jpeds.2014.12.069

3. Fruman DA, Chiu H, Hopkins BD, Bagrodia S, Cantley LC, Abraham RT. The PI3K Pathway in Human Disease. *Cell.* 2017;170(4):605-635. doi: 10.1016/j.cell.2017.07.029

4. Samuels Y, Wang Z, Bardelli A, Silliman N, Ptak J, Szabo S, Yan H, Gazdar A, Powell SM, Riggins GJ, Willson JK, Markowitz S, Kinzler KW, Vogelstein B, Velculescu VE. High frequency of mutations of the PIK3CA gene in human cancers. *Science.* 2004;304(5670):554. doi: 10.1126/science.1096502

5. Davare MA, Henderson JJ, Agarwal A, Wagner JP, Iyer SR, Shah N, Woltjer R, Somwar R, Gilheeney SW, DeCarvalo A, Mikkelson T, Van Meir EG, Ladanyi M, Druker BJ. Rare but Recurrent ROS1 Fusions Resulting From Chromosome 6q22 Microdeletions are Targetable Oncogenes in Glioma. *Clin Cancer Res.* 2018;24(24):6471-6482. doi: 10.1158/1078-0432.CCR-18-1052

6. Drilon A, Jenkins C, Iyer S, Schoenfeld A, Keddy C, Davare MA. ROS1-dependent cancers - biology, diagnostics and therapeutics. *Nat Rev Clin Oncol.* 2021;18(1):35-55. doi: 10.1038/s41571-020-0408-9

7. Juric D, Rodon J, Tabernero J, Janku F, Burris HA, Schellens JHM, Middleton MR, Berlin J, Schuler M, Gil-Martin M, Rugo HS, Seggewiss-Bernhardt R, Huang A, Bootle D, Demanse D, Blumenstein L, Coughlin C, Quadt C, Baselga J. Phosphatidylinositol 3-Kinase alpha-Selective Inhibition With Alpelisib (BYL719) in PIK3CA-Altered Solid Tumors: Results From the First-in-Human Study. *J Clin Oncol.* 2018;36(13):1291-1299. doi: 10.1200/JCO.2017.72.7107

8. Boscolo E, Coma S, Luks VL, Greene AK, Klagsbrun M, Warman ML, Bischoff J. AKT hyper-phosphorylation associated with PI3K mutations in lymphatic endothelial cells from a patient with lymphatic malformation. *Angiogenesis.* 2015;18(2):151-162. doi: 10.1007/s10456-014-9453-2

9. Cheng Y, Xu T, Li S, Ruan H. GPX1, a biomarker for the diagnosis and prognosis of kidney cancer, promotes the progression of kidney cancer. *Aging (Albany NY).* 2019;11(24):12165-12176. doi: 10.18632/aging.102555

10. Qiu QC, Wang L, Jin SS, Liu GF, Liu J, Ma L, Mao RF, Ma YY, Zhao N, Chen M, Lin BY. CHI3L1 promotes tumor progression by activating TGF-beta signaling pathway in hepatocellular carcinoma. *Sci Rep.* 2018;8(1):15029. doi: 10.1038/s41598-018-33239-8

11. Sirois I, Aguilar-Mahecha A, Lafleur J, Fowler E, Vu V, Scriver M, Buchanan M, Chabot C, Ramanathan A, Balachandran B, Legare S, Przybytkowski E, Lan C, Krzemien U, Cavallone L, Aleynikova O, Ferrario C, Guilbert MC, Benlimame N, Saad A, Alaoui-Jamali M, Saragovi HU, Josephy S, O'Flanagan C, Hursting SD, Richard VR, Zahedi RP, Borchers CH, Bareke E, Nabavi S, Tonellato P, Roy JA, Robidoux A, Marcus EA, Mihalcioiu C, Majewski J, Basik M. A Unique Morphological Phenotype in Chemoresistant Triple-Negative Breast Cancer Reveals Metabolic Reprogramming and PLIN4 Expression as a Molecular Vulnerability. *Mol Cancer Res.* 2019;17(12):2492-2507. doi: 10.1158/1541-7786.MCR-19-0264

12. Vadivel CK, Gluud M, Torres-Rusillo S, Boding L, Willerslev-Olsen A, Buus TB, Nielsen TK, Persson JL, Bonefeld CM, Geisler C, Krejsgaard T, Fuglsang AT, Odum N, Woetmann A. JAK3 Is Expressed in the Nucleus of Malignant T Cells in Cutaneous T Cell Lymphoma (CTCL). *Cancers (Basel).* 2021;13(2). doi: 10.3390/cancers13020280

13. Zhang Q, Zhang P, Li B, Dang H, Jiang J, Meng L, Zhang H, Zhang Y, Wang X, Li Q, Wang Y, Liu C, Li F. The Expression of Perilipin Family Proteins can be used as Diagnostic Markers of Liposarcoma and to Differentiate Subtypes. *J Cancer.* 2020;11(14):4081-4090. doi: 10.7150/jca.41736

14. Barclay SF, Inman KW, Luks VL, McIntyre JB, Al-Ibraheemi A, Church AJ, Perez-Atayde AR, Mangray S, Jeng M, Kreimer SR, Walker L, Fishman SJ, Alomari AI, Chaudry G, Trenor Iii CC, Adams D, Kozakewich HPW, Kurek KC. A somatic activating NRAS variant associated with kaposiform lymphangiomatosis. *Genet Med.* 2019;21(7):1517-1524. doi: 10.1038/s41436-018-0390-0

15. Croteau SE, Kozakewich HP, Perez-Atayde AR, Fishman SJ, Alomari AI, Chaudry G, Mulliken JB, Trenor CC, 3rd. Kaposiform lymphangiomatosis: a distinct aggressive lymphatic anomaly. *J Pediatr.* 2014;164(2):383-388. doi: 10.1016/j.jpeds.2013.10.013

16. Dummer R, Schadendorf D, Ascierto PA, Arance A, Dutriaux C, Di Giacomo AM, Rutkowski P, Del Vecchio M, Gutzmer R, Mandala M, Thomas L, Demidov L, Garbe C, Hogg D, Liszkay G, Queirolo P, Wasserman E, Ford J, Weill M, Sirulnik LA, Jehl V, Bozon V, Long GV, Flaherty K. Binimetinib versus dacarbazine in patients with advanced NRAS-mutant melanoma (NEMO): a multicentre, open-label, randomised, phase 3 trial. *Lancet Oncol.* 2017;18(4):435-445. doi: 10.1016/S1470-2045(17)30180-8

17. Venot Q, Blanc T, Rabia SH, Berteloot L, Ladraa S, Duong JP, Blanc E, Johnson SC, Hoguin C, Boccara O, Sarnacki S, Boddaert N, Pannier S, Martinez F, Magassa S, Yamaguchi J, Knebelmann B, Merville P, Grenier N, Joly D, Cormier-Daire V, Michot C, Bole-Feysot C, Picard A, Soupre V, Lyonnet S, Sadoine J, Slimani L, Chaussain C, Laroche-Raynaud C, Guibaud L, Broissand C, Amiel J, Legendre C, Terzi F, Canaud G. Targeted therapy in patients with PIK3CA-related overgrowth syndrome. *Nature.* 2018;558(7711):540-546. doi: 10.1038/s41586-018-0217-9

18. Mayer IA, Abramson VG, Formisano L, Balko JM, Estrada MV, Sanders ME, Juric D, Solit D, Berger MF, Won HH, Li Y, Cantley LC, Winer E, Arteaga CL. A Phase Ib Study of Alpelisib (BYL719), a PI3Kalpha-Specific Inhibitor, with Letrozole in ER+/HER2- Metastatic Breast Cancer. *Clin Cancer Res.* 2017;23(1):26-34. doi: 10.1158/1078-0432.CCR-16-0134

19. Janku F, Hong DS, Fu S, Piha-Paul SA, Naing A, Falchook GS, Tsimberidou AM, Stepanek VM, Moulder SL, Lee JJ, Luthra R, Zinner RG, Broaddus RR, Wheler JJ, Kurzrock R. Assessing PIK3CA and PTEN in early-phase trials with PI3K/AKT/mTOR inhibitors. *Cell Rep.* 2014;6(2):377-387. doi: 10.1016/j.celrep.2013.12.035

20. Juric D, Krop I, Ramanathan RK, Wilson TR, Ware JA, Sanabria Bohorquez SM, Savage HM, Sampath D, Salphati L, Lin RS, Jin H, Parmar H, Hsu JY, Von Hoff DD, Baselga J. Phase I Dose-Escalation Study of Taselisib, an Oral PI3K Inhibitor, in Patients with Advanced Solid Tumors. *Cancer Discov.* 2017;7(7):704-715. doi: 10.1158/2159-8290.CD-16-1080

21. Di Nicolantonio F, Arena S, Tabernero J, Grosso S, Molinari F, Macarulla T, Russo M, Cancelliere C, Zecchin D, Mazzucchelli L, Sasazuki T, Shirasawa S, Geuna M, Frattini M, Baselga J, Gallicchio M, Biffo S, Bardelli A. Deregulation of the PI3K and KRAS signaling pathways in human cancer cells determines their response to everolimus. *J Clin Invest.* 2010;120(8):2858-2866. doi: 10.1172/JCI37539

22. Freixo C, Ferreira V, Martins J, Almeida R, Caldeira D, Rosa M, Costa J, Ferreira J. Efficacy and safety of sirolimus in the treatment of vascular anomalies: A systematic review. *J Vasc Surg.* 2020;71(1):318-327. doi: 10.1016/j.jvs.2019.06.217

23. Hucthagowder V, Shenoy A, Corliss M, Vigh-Conrad KA, Storer C, Grange DK, Cottrell CE. Utility of clinical high-depth next generation sequencing for somatic variant detection in the PIK3CA-related overgrowth spectrum. *Clin Genet.* 2017;91(1):79-85. doi: 10.1111/cge.12819

24. Bendell JC, Rodon J, Burris HA, de Jonge M, Verweij J, Birle D, Demanse D, De Buck SS, Ru QC, Peters M, Goldbrunner M, Baselga J. Phase I, dose-escalation study of BKM120, an oral pan-Class I PI3K inhibitor, in patients with advanced solid tumors. *J Clin Oncol.* 2012;30(3):282-290. doi: 10.1200/JCO.2011.36.1360

25. Hong DS, Bowles DW, Falchook GS, Messersmith WA, George GC, O'Bryant CL, Vo AC, Klucher K, Herbst RS, Eckhardt SG, Peterson S, Hausman DF, Kurzrock R, Jimeno A. A multicenter phase I trial of PX-866, an oral irreversible phosphatidylinositol 3-kinase inhibitor, in patients with advanced solid tumors. *Clin Cancer Res.* 2012;18(15):4173-4182. doi: 10.1158/1078-0432.CCR-12-0714

26. Juric D, Castel P, Griffith M, Griffith OL, Won HH, Ellis H, Ebbesen SH, Ainscough BJ, Ramu A, Iyer G, Shah RH, Huynh T, Mino-Kenudson M, Sgroi D, Isakoff S, Thabet A, Elamine L, Solit DB, Lowe SW, Quadt C, Peters M, Derti A, Schegel R, Huang A, Mardis ER, Berger MF, Baselga J, Scaltriti M. Convergent loss of PTEN leads to clinical resistance to a PI(3)Kalpha inhibitor. *Nature.* 2015;518(7538):240-244. doi: 10.1038/nature13948

27. Akhavanfard S, Padmanabhan R, Yehia L, Cheng F, Eng C. Comprehensive germline genomic profiles of children, adolescents and young adults with solid tumors. *Nat Commun.* 2020;11(1):2206. doi: 10.1038/s41467-020-16067-1

28. Mustjoki S, Young NS. Somatic Mutations in "Benign" Disease. *N Engl J Med.* 2021;384(21):2039-2052. doi: 10.1056/NEJMra2101920

29. Castel P, Carmona FJ, Grego-Bessa J, Berger MF, Viale A, Anderson KV, Bague S, Scaltriti M, Antonescu CR, Baselga E, Baselga J. Somatic PIK3CA mutations as a driver of sporadic venous malformations. *Sci Transl Med.* 2016;8(332):332ra342. doi: 10.1126/scitranslmed.aaf1164

30. Castillo SD, Tzouanacou E, Zaw-Thin M, Berenjeno IM, Parker VE, Chivite I, Mila-Guasch M, Pearce W, Solomon I, Angulo-Urarte A, Figueiredo AM, Dewhurst RE, Knox RG, Clark GR, Scudamore CL, Badar A, Kalber TL, Foster J, Stuckey DJ, David AL, Phillips WA, Lythgoe MF, Wilson V, Semple RK, Sebire NJ, Kinsler VA, Graupera M, Vanhaesebroeck B. Somatic activating mutations in Pik3ca cause sporadic venous malformations in mice and humans. *Sci Transl Med.* 2016;8(332):332ra343. doi: 10.1126/scitranslmed.aad9982

31. Limaye N, Kangas J, Mendola A, Godfraind C, Schlogel MJ, Helaers R, Eklund L, Boon LM, Vikkula M. Somatic Activating PIK3CA Mutations Cause Venous Malformation. *Am J Hum Genet.* 2015;97(6):914-921. doi: 10.1016/j.ajhg.2015.11.011

32. Ren AA, Snellings DA, Su YS, Hong CC, Castro M, Tang AT, Detter MR, Hobson N, Girard R, Romanos S, Lightle R, Moore T, Shenkar R, Benavides C, Beaman MM, Müller-Fielitz H, Chen M, Mericko P, Yang J, Sung DC, Lawton MT, Ruppert JM, Schwaninger M, Körbelin J, Potente M, Awad IA, Marchuk DA, Kahn ML. PIK3CA and CCM mutations fuel cavernomas through a cancer-like mechanism. *Nature.* 2021. doi: 10.1038/s41586-021-03562-8

33. Rafnar T, Gunnarsson B, Stefansson OA, Sulem P, Ingason A, Frigge ML, Stefansdottir L, Sigurdsson JK, Tragante V, Steinthorsdottir V, Styrkarsdottir U, Stacey SN, Gudmundsson J, Arnadottir GA, Oddsson A, Zink F, Halldorsson G, Sveinbjornsson G, Kristjansson RP, Davidsson OB, Salvarsdottir A, Thoroddsen A, Helgadottir EA, Kristjansdottir K, Ingthorsson O, Gudmundsson V, Geirsson RT, Arnadottir R, Gudbjartsson DF, Masson G, Asselbergs FW, Jonasson JG, Olafsson K, Thorsteinsdottir U, Halldorsson BV, Thorleifsson G, Stefansson K. Variants associating with uterine leiomyoma highlight genetic background shared by various cancers and hormone-related traits. *Nat Commun.* 2018;9(1):3636. doi: 10.1038/s41467-018-05428-6

34. Gallagher CS, Makinen N, Harris HR, Rahmioglu N, Uimari O, Cook JP, Shigesi N, Ferreira T, Velez-Edwards DR, Edwards TL, Mortlock S, Ruhioglu Z, Day F, Becker CM, Karhunen V, Martikainen H, Jarvelin MR, Cantor RM, Ridker PM, Terry KL, Buring JE, Gordon SD, Medland SE, Montgomery GW, Nyholt DR, Hinds DA, Tung JY, andMe Research T, Perry JRB, Lind PA, Painter JN, Martin NG, Morris AP, Chasman DI, Missmer SA, Zondervan KT, Morton CC. Genome-wide association and epidemiological analyses reveal common genetic origins between uterine leiomyomata and endometriosis. *Nat Commun.* 2019;10(1):4857. doi: 10.1038/s41467-019-12536-4

35. Fritsche LG, Gruber SB, Wu Z, Schmidt EM, Zawistowski M, Moser SE, Blanc VM, Brummett CM, Kheterpal S, Abecasis GR, Mukherjee B. Association of Polygenic Risk Scores for Multiple Cancers in a Phenome-wide Study: Results from The Michigan Genomics Initiative. *Am J Hum Genet.* 2018;102(6):1048-1061. doi: 10.1016/j.ajhg.2018.04.001

36. Sanders MGH, Pardo LM, Uitterlinden AG, Smith AM, Ginger RS, Nijsten T. The Genetics of Seborrheic Dermatitis: A Candidate Gene Approach and Pilot Genome-Wide

Association Study. *J Invest Dermatol.* 2018;138(4):991-993. doi: 10.1016/j.jid.2017.11.020

37. Anglesio MS, Papadopoulos N, Ayhan A, Nazeran TM, Noe M, Horlings HM, Lum A, Jones S, Senz J, Seckin T, Ho J, Wu RC, Lac V, Ogawa H, Tessier-Cloutier B, Alhassan R, Wang A, Wang Y, Cohen JD, Wong F, Hasanovic A, Orr N, Zhang M, Popoli M, McMahon W, Wood LD, Mattox A, Allaire C, Segars J, Williams C, Tomasetti C, Boyd N, Kinzler KW, Gilks CB, Diaz L, Wang TL, Vogelstein B, Yong PJ, Huntsman DG, Shih IM. Cancer-Associated Mutations in Endometriosis without Cancer. *N Engl J Med.* 2017;376(19):1835-1848. doi: 10.1056/NEJMoa1614814

38. Gagnier JJ, Kienle G, Altman DG, Moher D, Sox H, Riley D, Group C. The CARE guidelines: consensus-based clinical case reporting guideline development. *BMJ Case Rep.* 2013;2013. doi: 10.1136/bcr-2013-201554

Supplementary Table 1. Somatic coding mutations identified from whole genome sequencing

Gene_Name	Protein_Change	VAF	alt_depth	ref_depth	COSMIC
HRNR 0.105	p.T616A	0.105	4	51	
OR2T3	p.S247F	0.171	8	53	
PLXDC2	p.V396I	0.167	4	22	
FOLH1	p.R190W	0.333	8	20	
IPO8	p.M488fs	0.125	3	28	
KRR1	p.R134Q	0.188	3	17	
KRTAP4-11	p.L161V	0.116	9	49	
TTYH1	p.E440fs	0.130	6	31	
TTYH1	p.440_441insH	0.130	6	30	
KIF5C	p.K151fs	0.200	3	16	
LY75-CD302	p.T1393I	0.188	3	18	
BARD1	p.P24S	0.087	4	59	
KRTAP10-12	p.P92S	0.133	5	38	
NFXL1	p.P246L	0.176	3	20	
PLA2G7	p.R92H	0.188	3	18	
NAT2	p.R268K	0.200	7	28	p.R268K
AQP7	p.Y64F	0.068	7	88	
KIAA1984	p.N421T	0.125	4	42	

The genetic coding variants that exist in LM but do not exist in germline DNA. These pass MuTect2 quality filters (designed to call somatic variants only) and have three or more alternate reads. VAF, Variant Allele Frequency; COSMIC, Catalogue Of Somatic Mutations In Cancer.